Highly Branched Waxy Potato Starch-Based Polyelectrolyte

Fan, Yifei; Bose, Ranjita K.; Picchioni, Francesco

Published in:
Industrial and Engineering Chemistry Research

DOI:
10.1021/acs.iecr.9b06893

Publication date:
2020

I&EC research
Industrial & Engineering Chemistry Research

pubs.acs.org/IECR

Article

Highly Branched Waxy Potato Starch-Based Polyelectrolyte: Controlled Synthesis and the Influence of Chain Composition on Solution Rheology

Yifei Fan, Ranjita K. Bose, and Francesco Picchioni*

Cite This: *Ind. Eng. Chem. Res.* 2020, 59, 10847−10856

Read Online

ACCESS | Metrics & More | Article Recommendations | Supporting Information

ABSTRACT: In the present work, a series of highly branched random copolymers of acrylamide (AM), sodium 2-acrylamido-2-methyl-1-propanesulfonate (SAMPS), and *N*-isopropylacrylamide (NIPAM) were prepared by using water-soluble waxy potato starch-based macroinitiator via aqueous Cu^0-mediated living radical polymerization (25 °C). The AM/SAMPS/NIPAM ratio was varied to investigate the influence of chain composition on the aqueous rheological properties of the prepared copolymers. Rheological results indicated an optimum SAMPS intake (25 mol %) for the balanced performance of viscosity and salt resistance in saline water. The intake of NIPAM units (e.g., 25 mol %), contrary to what was expected, undermines the thickening ability of the copolymers in saline water because of hydrophobic association. In high salinity solution, thermo-thickening behavior can be observed at low shear rates ($\gamma \leq 3\ s^{-1}$) because of the screening effect of salt on the negatively charged SAMPS units. At the high shear rate, the thermo-thickening behavior disappears because of the disruption of the NIPAM aggregates. These results pave the way toward the use of the prepared polymers as rheology modifiers in a variety of possible formulations for different applications, in particular in enhanced oil recovery.

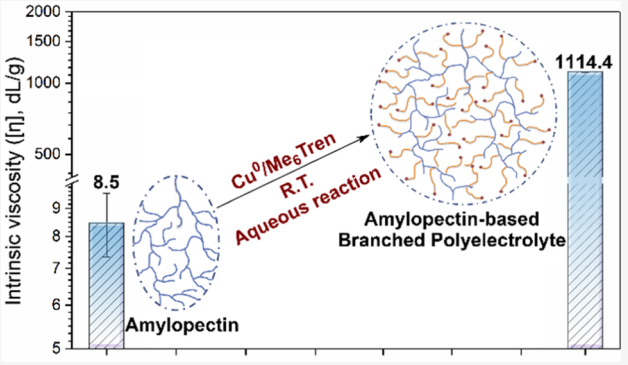

1. INTRODUCTION

Enhanced oil recovery (EOR) is a widely used technique to promote oil production because of the increasing demand for oil and the relatively large portion (~40% of original oil) of unexploited residual oil.[1] Polymer flooding is one common EOR method entailing the use of a polymer as a thickener to reduce the mobility difference between water and oil and thus increase the sweep efficiency of water on the porous structure, where crude oil is deposited. Partially hydrolyzed polyacrylamide (HPAM) has been widely used in recent decades for polymer flooding because of its low cost.[2,3] However, HPAM tends to hydrolyze and precipitate out in the reservoirs, especially in those with high temperatures (up to 130 °C) and salinity (up to 200,000 ppm, in particular when divalent cations such as Ca^{2+} and Mg^{2+} are present).[4−6] This is detrimental to the performance of polymer flooding and also harmful to the reservoir. In this case, carefully designed polymers, which can withstand the hostile (saline) environment, are needed for sustainable exploration. Another problem in the oilfield exploitation is the management of produced water which is a byproduct with a large volume. This kind of water usually contains a variety of organic and inorganic pollutants such as hydrocarbons, heavy metals, chemicals during drilling, and in most cases also has high salinity.[7] Reinjection of produced water for EOR is one attractive option for the sake of the environment (fragile ecosystems such as offshore and Arctic areas) and reservoir protection (the use of a different water source might result in the significant formation of precipitated salts, thus damaging the reservoir exploration).[8] The utilization of saline-resistant polymers may be helpful to achieve this purpose.

The salt-resistance of polymers, like many other properties, is also affected by both their composition and structure. For example, our previous studies revealed that branched structures can result in higher viscosity and better viscoelastic properties than linear ones because of their more stable hydrodynamic volume inherent to the steric hindrance in the structure.[9−11] As a matter of fact, copolymers based on the homogeneous grafting of highly branched waxy potato starch did display both thermo-thickening behavior and stable viscosity profile in different saline solutions.[12−15] However, efforts are still needed

Received: December 16, 2019
Revised: May 11, 2020
Accepted: May 13, 2020
Published: May 13, 2020

https://dx.doi.org/10.1021/acs.iecr.9b06893
Ind. Eng. Chem. Res. 2020, 59, 10847−10856

to improve the solubility (dissolve faster) and viscosity of copolymers compared with that of commercial HPAM products. One option is the incorporation of salt-resistant polyelectrolyte segments in the highly branched structure. Poly(2-acrylamido-2-methyl-1-propanesulfonic acid sodium salts) (PAMPS), as an anionic polyelectrolyte bearing negative charges in polymer chains such as HPAM, is reported to be more stable at high temperature in saline water.[16,17] Moreover, PAMPS polymers are now also recognized as potential materials for bioengineering,[18] forward osmosis,[19,20] and catalyst support for energy and environment applications.[21] Thus, the synthesis of PAMPS and its copolymers has been an interesting research topic in recent years.[22−25]

In the case of grafting PAMPS (co)polymers onto starch, generally, the reaction is carried out in water by free radical polymerization with ceric salts as the initiator.[23,26] As reported, by using controlled polymerization, such as transition-metal [mainly Cu(I)]-mediated atom transfer radical polymerization (ATRP), Cu^0-mediated aqueous living radical polymerization (Cu^0-mediated LRP), and reversible addition−fragmentation chain transfer (RAFT), the formation of homopolymer, typical for conventional free radical polymerization, can be avoided and tailor-made properties can be achieved.[12,22,23] This is favorable for the investigation of the influence of chain length and structure on polymer properties. Compared with RAFT, which usually should be carried out above 50 °C, and normal ATRP, Cu^0-mediated LRP could be achieved at room temperature or even lower (e.g., 0 °C) while maintaining a much higher polymerization rate in aqueous solution.[27] However, reports on the synthesis of PAMPS and its copolymers by Cu^0-mediated LRP are still rare compared with RAFT and "classical" ATRP.[24,28−30]

In the present study, the controllability of Cu^0-mediated LRP on the synthesis of poly(sodium 2-acrylamido-2-methyl-1-propanesulfonate) (PSAMPS) in water was verified. Then, a water-soluble macroinitiator was synthesized by homogeneous esterification of waxy potato starch with 2-bromopropionyl bromide (BpB) in *N*,*N*-dimethylacetamide (DMAc).[31,32] Based on this, a series of branched random copolymers of acrylamide (AM), sodium 2-acrylamido-2-methyl-1-propanesulfonate (SAMPS), and *N*-isopropylacrylamide (NIPAM) were prepared by aqueous Cu^0-mediated living radical polymerization (Cu^0-mediated LRP) at room temperature (illustration see Figure S1). The macroinitiator and polymers were characterized by nuclear magnetic resonance (NMR) and Fourier transform infrared (FT-IR). For potential applications such as EOR, the ratios of the three monomers were varied to study the influence of chain composition on the rheological properties of polymer solutions and their response to temperature and saline water.

2. MATERIALS AND METHODS

2.1. Materials. Waxy potato starch (>95% amylopectin) was kindly donated by Avebe (the Netherlands) and dried under vacuum at 60 °C for 48 h before use. Lithium chloride from Sigma-Aldrich was dried under vacuum at 80 °C for 24 h before use. Copper powder (<75 μm) from Sigma-Aldrich was stored under a N_2 atmosphere. Anhydrous DMAc, 2-bromopropionic acid, BpB, formaldehyde solution (37%), formic acid (>95%), and AM were purchased from Sigma-Aldrich and used as received. 2-Acrylamido-2-methyl-1-propanesulfonic acid (AMPS) was purchased from Sigma-Aldrich and neutralized with sodium hydroxide (from Sigma-Aldrich) in Milli-Q solution which was then poured into tenfold acetone (cooled with an ice bath) to obtain the solid SAMPS. Tris(2-aminoethyl)amine (Tren) was purchased from TCI and used as received for the synthesis of tris[2-(dimethylamino)ethyl]amine(Me_6Tren) following the procedures reported.[33] NIPAM (stabilized with MEHQ) from TCI was recrystallized from acetone to remove the inhibitor.

2.2. Characterization. The composition of the synthesized copolymer was determined by an Elementar vario MICRO cube CHNS elemental analyzer. For a starch-based grafted copolymer without NIPAM intake, samples were taken after Soxhlet extraction as the trace solvent (ethanol) impurities have no influence on the result. For the NIPAM containing copolymers, samples from the Soxhlet extraction were dissolved in Milli-Q water and rotovap was used to remove the trace solvent. The obtained samples were freeze-dried for one day before the test. The ratio of monomer units can be obtained according to the following equation

$$\gamma(\mathrm{SAMPS}) = \frac{14 \times S\ \%}{32 \times N\ \%} \tag{1}$$

$$\gamma(\mathrm{AM}) = \frac{1}{3} \times \left(6 - \frac{14 \times C\ \%}{12 \times N\ \%} + \frac{14 \times S\ \%}{32 \times N\ \%}\right) \tag{2}$$

where γ(SAMPS) and γ(AM) stand for the mole ratio of SAMPS and AM in the copolymer, respectively, *C* %, *N* %, and *S* % is the mass ratio of carbon, nitrogen, and sulfur in the copolymer, respectively (see Table S1).

A Varian Mercury Plus 400 MHz spectrometer was employed for the recording of NMR spectra with deuterated water from Sigma-Aldrich as the solvent. FT-IR spectra were obtained via an IRTracer-100 SHIMADZU FT-IR spectrophotometer equipped with attenuated total reflection accessories and LabSolutions IR software. An Agilent 1200 aqueous gel permeation chromatography (GPC) system equipped with a differential refractive index detector and Polymer Standard Service (PSS) column set (PSS SUPREMA 100, 1000, 3000 Å) was used for the characterization of molecular weight and distributions. The mobile phase used was 0.05 M $NaNO_3$ aqueous solution with a flow rate of 1 mL/min. The system temperature was regulated to 40 °C. Polyethylene oxide standards (ReadyCal, M_p 200−1,200,000) from Fluka were used for calibration. Samples were filtered through a Teflon membrane with 0.22 μm pore size before injection. The experimental molecular weight and polydispersity index (PDI) of synthesized polymers were determined via Agilent GPC/size exclusion chromatography software.

A HAAKE Mars III (Thermo Scientific) rheometer equipped with a cone-and-plate geometry (diameter 60 mm, angle 2°) was employed for the characterization of rheological properties of polymer solutions. The viscosity of polymer solution was measured as a function of shear rate (0.1 to 1750 s^{-1}, T = 20 °C), salt concentration (5000−100,000 ppm of NaCl, T = 20 °C, shear rate 10 s^{-1}), and temperature (10 to 95 °C, shear rate 1, 3 and 10 s^{-1}), respectively.

Martin equation was used to determine the intrinsic viscosity of polymer solutions[34]

$$\eta_{\mathrm{red}} = \frac{\eta_{\mathrm{sp}}}{c} = [\eta]\mathrm{e}^{\kappa_M c[\eta]} \tag{3}$$

where η_{red} is the reduced viscosity, η_{sp} is the specific viscosity, c is the polymer concentration, $[\eta]$ is the intrinsic viscosity, and k_M is a constant that depends on the polymer−solvent system.

https://dx.doi.org/10.1021/acs.iecr.9b06893
Ind. Eng. Chem. Res. 2020, 59, 10847−10856

The Carreau-Yasuda model was used for the determination of relaxation time (λ)[9,35,36]

$$\frac{\eta - \eta_\infty}{\eta_0 - \eta_\infty} = [1 + (\lambda \cdot \gamma)^\alpha]^{n-1/\alpha} \quad (4)$$

where η is the viscosity, η_0 is the zero shear rate viscosity, η_∞ is the viscosity at the infinite shear rate, $1/\lambda$ is the critical shear rate for the onset of shear thinning, $n-1$ is the power-law index, and α represents the transition region between η_0 and the power-law region.

2.3. Synthesis of Starch-Based Macroinitiator. Waxy potato starch (1.30 g, 8 mmol) and lithium chloride (0.51 g, 12 mmol) were added to a 100 mL three-necked flask (dried at 100 °C for 12 h before use) equipped with a mechanical stirrer. The oxygen and residual water in the system were removed via three evacuate−refill cycles under heat with N_2. Anhydrous DMAc (50 mL) was injected to the flask and the mixture was stirred at 130 °C for about 1 h under a N_2 atmosphere then cooled down to obtain a transparent solution. BpB (0.21 mL, 2 mmol) was added dropwise within 15 min to the starch solution cooled with an ice bath under the protection of N_2. The reaction mixture was then stirred for 3 h at room temperature. The crude product was precipitated out with tenfold acetone and filtered, washed then dried under vacuum at 45 °C for 24 h. The obtained white powder was further purified by Soxhlet extraction with acetone as the solvent for 24 h and the final yield was 87%.

2.4. Synthesis of Starch-Based Copolymers by Aqueous Cu^0-Mediated LRP. *2.4.1. Typical Polymerization Protocol.* H_2O (50 mL), starch-based macroinitiator (StBr) (24.3 mg, 0.02 mmol), a mixture of AM and SAMPS (120 mmol in total), together with Me_6TREN (12 μL, 0.04 mmol) were charged to a 100 mL three-neck round-bottom flask then deoxygenated by three freeze pump thaw cycles. Cu powder (2.6 mg, 0.04 mmol) was added subsequently with rapid stirring under the protection of nitrogen. The reaction mixture was stirred at room temperature for 15 min. The copolymer was separated out via freeze-drying the reaction solution and followed by Soxhlet extraction with ethanol as the solvent for 48 h. The pure product was then vacuum dried at 65 °C for 48 h. For the purpose of short and clear, starch-g-Poly(AM-*co*-NIPAM-*co*-SAMPS) copolymers were named as ANS0000 and ANS1510 and so forth, in which the four digits stand for the ratio of NIPAM (N) and SAMPS (S) in the feeding solution, respectively (details see Table 2).

2.5. Cleaving of Graft Polymer Chains from the Starch Backbone. Starch-based copolymer (0.10 g) was dissolved in 10 mL Milli-Q water in a round-bottom flask together with 0.10 mL concentrated hydrochloric acid. The reaction mixture was stirred and refluxed at 100 °C for 3 h. The resulting free (co)polymer was precipitated out and washed with acetone three times then dried under vacuum at 60 °C for 24 h.

3. RESULTS AND DISCUSSION

The successful synthesis of a water-soluble waxy potato StBr was proved by FT-IR and NMR (^{1}H-NMR, ^{13}C-NMR, and gHSQC). Details can be found in the Supporting Information (Figures S2 and S3).

Compared with the synthesis of low degree of polymerization (DP) polymer, normally a higher catalyst/initiator ratio is needed to obtain a high DP polymer with controlled Cu^0-mediated LRP. This is in agreement with the literature.[27] As shown in Table 1, linear PSAMPS (co)polymers were synthesized with different DP (at different catalyst/initiator ratio) to verify the control on the Cu^0-mediated LRP polymerization. PDI values in Table 1 suggest a relatively narrow distribution of (co)polymers, which constitutes a proof of controlled polymerization.

Table 1. Experimental Data of Linear PSAMPS (co)polymer Synthesized by Cu^0-Mediated LRP

sample	[M]:[L]:[Cu^0]:[L]	monomer ratio[a]	ratio (SAMPS)	DP[c]	PDI[d]
entry 1	50:1:0.6:0.6	100:0:0	100	46	1.32
entry 2	500:1:1:0.8	100:0:0		N.A.	
entry 3	500:1:2:2	100:0:0	100	390	1.47
entry 4	2000:1:2:2	75:0:25	23.5[b]	1178	1.45

[a]The ratio of AM/NIPAM/SAMPS in feeding solution. [b]The composition of copolymer determined by elemental analysis, data see support information (Table S1). [c]The DP determined according to NMR and mass, N.A. means no reaction. [d]The PDI determined by GPC.

For homopolymers, the kinetic of polymerization was also monitored by ^{1}H-NMR and the kinetic plots (Figure 1) were thus obtained according to eq 5.[37]

$$\mathrm{Ln}(M_0/M_t) = k_p(R_i/k_t)^{1/2} \cdot t \quad (5)$$

where M_0 and M_t are the monomer concentration at the beginning of polymerization and at time t, respectively, k_p indicates the kinetic propagation constant, R_i the initiation rate while k_i the termination rate constant. Clearly, the linear relationship between $\ln(M_0/M_t)$ and t in Figure 1 reveals a reasonably controlled polymerization, which is in line with the PDI values from GPC (Table 1). Besides, the conversion and kinetic curves also indicate an induction period in polymerization which is attributed to the absence of soluble copper species (Cu^I and Cu^{II} species) at the beginning of polymerization.[38] Briefly, the Cu^I is also an efficient activator to accelerate the polymerization progress but its accumulation in the system via initial Cu^0 activation and Cu^{II} disproportionation afterward (Scheme 1) needs time which is observed as the induction period.

A series of St-g-poly(AM-*co*-NIPAM-*co*-SAMPS) (ANS copolymers) with different NIPAM and SAMPS molar intake were then synthesized by Cu^0-mediated LRP with StBr as the initiator and copper powder/Me_6Tren as the catalyst system (Table 2). Information for the synthesis of St-g-poly(AM-*co*-NIPAM) (ANS1000 and ANS2500) is also listed in Table 2 for the clarity of discussion, details about these two copolymers are available in our previous report.[12]

According to our previous work, the target DP for all the samples was set to 6000 to achieve satisfactory viscosity values for potential applications such as EOR. The copolymers synthesized in the present work were characterized by FT-IR (Figure 2a) and ^{1}H-NMR (Figure 2b). The absorption peak around 3188 cm^{-1} in FT-IR spectrums was assigned to the stretch of the N−H bond in the amide group. For the ANS0000, a typical amide group peaks at 1652 cm^{-1} (amide I) and 1610 cm^{-1} (amide II) could also be seen in the spectrum. With the increase of SAMPS and (or) NIPAM intake in the copolymer, the amide I and II peaks gradually shifted to 1628 and 1530 cm^{-1}, respectively.[39] The symmetrical and asym-

https://dx.doi.org/10.1021/acs.iecr.9b06893
Ind. Eng. Chem. Res. 2020, 59, 10847−10856

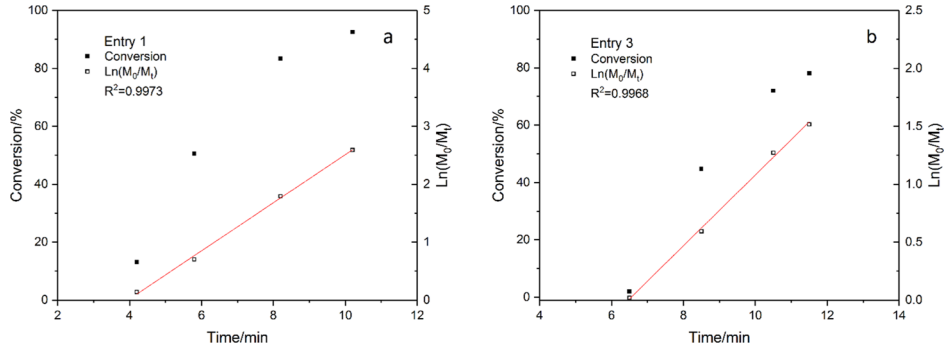

Figure 1. Kinetic plot of the PSAMPS homopolymer synthesized by Cu^0-mediated LRP.

Scheme 1. Proposed Reaction Kinetic in Cu^0-Mediated LRP (Adapted with Permission from Ref 38 Copyright 2015 Royal Society of Chemistry)

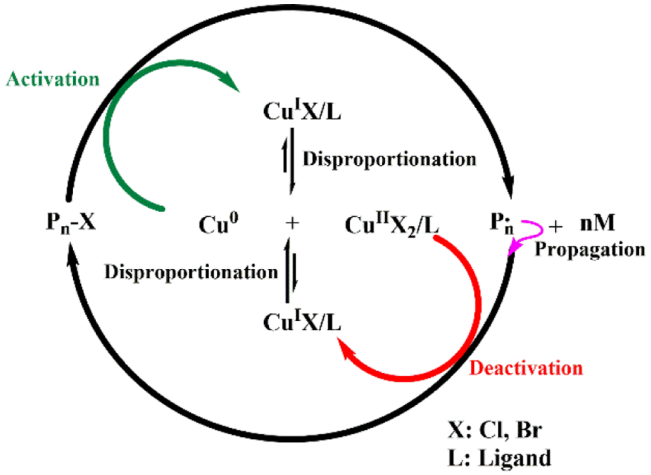

metrical stretch of the S═O bond in the sulfonate group could also be seen at 1040 and 1180 cm^{-1}, respectively.[40] The ^{1}H-NMR spectra of the copolymers are shown in Figure 2b, in which the peak around 1.0 ppm was attributed to the methyl protons in the NIPAM unit while the peak around 1.3 ppm was attributed to the methyl protons in the SAMPS unit. The peak at 3.8 ppm originates from the tertiary carbon protons in the NIPAM amide group while the broad peak in the range of 3.0−3.5 ppm originates from the SAMPS methine carbon (connected with the sulfonic group) protons. The signals in the range of 1.9−2.3 ppm and 1.2−1.8 ppm (partially overlap with the peak from SAMPS methyl protons) were assigned to the tertiary and secondary carbon protons in the copolymer backbone, respectively.

As shown in Table 2, the mole ratio of SAMPS and NIPAM in the feeding monomer mixture were varied from 0 to 50 and 0 to 25%, respectively, while the overall target DP was set to 6000 for all the copolymer. Elemental analysis, instead of NMR due to the overlapping peaks in the spectra, was used to determine the mole percentage of the SAMPS unit (for all copolymers) and AM unit (for copolymers with NIPAM) in the product according to eqs 1 and 2 (see the Materials and Methods section).

The polymerization kinetics were not monitored because of the relatively high rate and corresponding high solution viscosity. However, the controllability of Cu^0-mediated LRP on the grafting can be verified, although indirectly, by the PDI (obtained from GPC) of the (co)polymer cleaved from the starch backbone. As shown in Table 2, narrow molecular weight distribution (PDI < 1.6) which suggests a reasonably controlled polymerization is observed after the hydrolyzation of the starch backbone. Similar to the GPC traces shown in other reports,[41,42] the (co)polymers cleaved from the starch backbone also display a non-normal distribution (Figure S4). Given the rheology test results shown below, the copolymer with higher hydrodynamic volume (thus higher viscosity) displays larger deviation from normal distribution which might be explained by the residual "deactivation by propagation" as proposed in the literature.[43] Accordingly, although the "gel effect" at high conversion constrains the movement of polymer chains and thus results in the inefficient control on molecular

Table 2. Experimental Data of Starch-Based Grafted Copolymer Synthesized by Cu^0-Mediated LRP

			conversion/%[b]			ratio[c]			
sample	monomer ratio[a]	time/min	AM	NIPAM	SAMPS	NIPAM	SAMPS	DP[b]	PDI[d]
ANS0000	100:0:0	12	91.56					5554	1.42
ANS0010	90:0:10	12	96.95		94.80		9.8	5804	1.47
ANS1000	90:10:0	12	80.66	80.66		10.0		4840	1.64
ANS0025	75:0:25	15	90.67		90.19		24.9	5433	1.51
ANS2500	75:25:0	15	92.57	82.95		23.0		5410	[e]
ANS1015	75:10:15	15	89.55	91.96	90.26	10.2	15.1	5394	1.54
ANS2525	50:25:25	20	86.19	95.34	85.26	27.0	24.2	5295	[e]
ANS0050	50:0:50	18	92.25		83.80		47.6	5282	1.53

[a]The ratio of AM/NIPAM/SAMPS: in feeding solution. Overall ratio for the grafting [M]:[I]:[Cu^0]:[L] = 6000:1:2:2. [b]Monomer conversion and polymer DP determined by elemental analysis (or NMR) and mass. [c]The composition of grafted chains determined according to elemental analysis or NMR. [d]The PDI of the copolymer after the hydrolyzation of starch backbone. [e]Not available due to potential high intermolecular association, leading to retention of the polymer inside the GPC column.

https://dx.doi.org/10.1021/acs.iecr.9b06893
Ind. Eng. Chem. Res. 2020, 59, 10847−10856

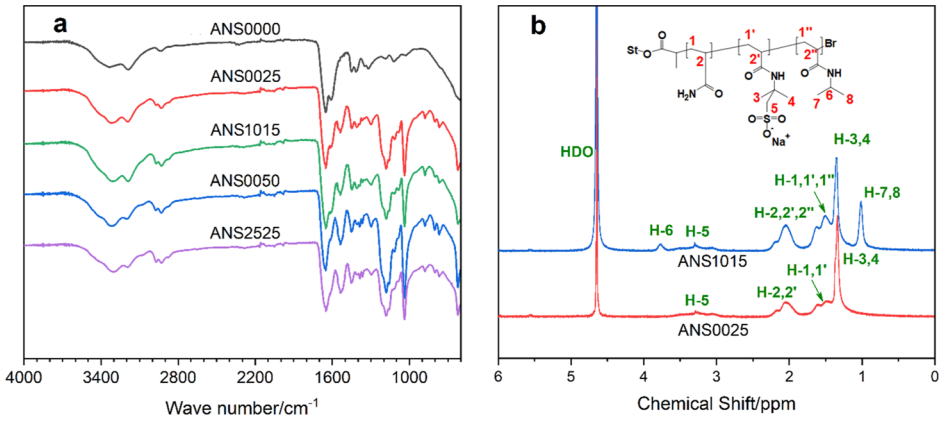

Figure 2. FT-IR (a) and ^{1}H-NMR (b) spectrum of starch-based graft copolymers.

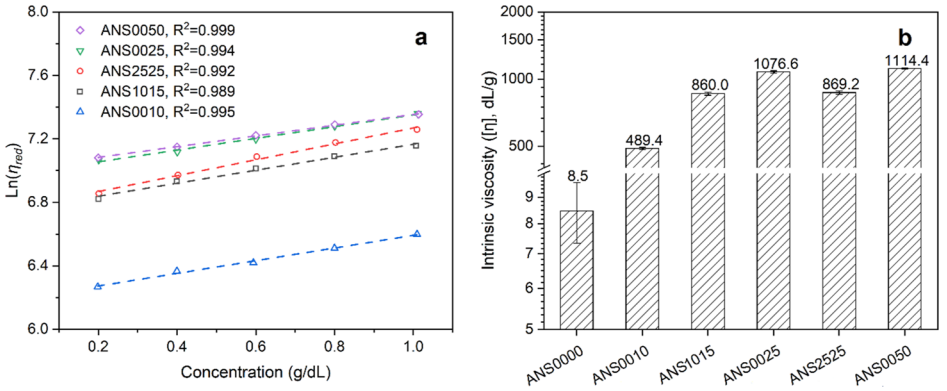

Figure 3. Reduced viscosity as a function of polymer concentration (Martin equation) (a) and corresponding intrinsic viscosity (b).

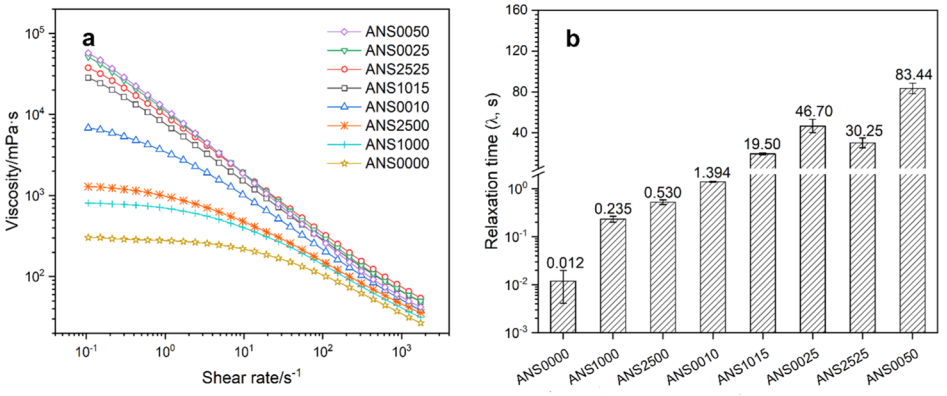

Figure 4. Viscosity as a function of shear rate (a, 1.2 wt % copolymer solution) and corresponding relaxation time from Carreau−Yasuda model (b).

weight, the activation/deactivation cycle can still be maintained because of the diffusion of activation/deactivation species. Moreover, the radical centers can also "reach" the deactivation species by propagation (residual deactivation) which is helpful to lower the PDI.

To investigate the influence of chain composition on copolymer solution properties, a series of rheology tests were carried out. For a polymer with a given molecular structure, the intrinsic viscosity is an indication of the hydrodynamic volume of polymers.[44,45] The intrinsic viscosity can be obtained by extrapolating the plot of $\ln(\eta_{red})$ against polymer concentration to $c = 0$ (see the Materials and Methods section). It should be noted that for linear polyelectrolytes the electrostatic repulsion expands the macromolecule coil in dilute solution because of intramolecular repulsion but compresses that in higher concentration because of intermolecular repulsion. As a result, higher reduced viscosity can be observed at a lower polymer concentration (known as polyelectrolyte effect). This makes the extrapolation to infinite dilution quite unreliable, so the measurements for linear polyelectrolyte usually are carried out in a salt solution (such as 0.1 M NaCl) to screen out the influence of charges.[46,47] However, this makes the comparison between samples inconvenient as the salt concentration varies in order to effectively shield different charge density, while the final result is also related to the salt concentration.[48] Furthermore, in the case of highly branched polyelectrolytes,

https://dx.doi.org/10.1021/acs.iecr.9b06893
Ind. Eng. Chem. Res. 2020, 59, 10847−10856

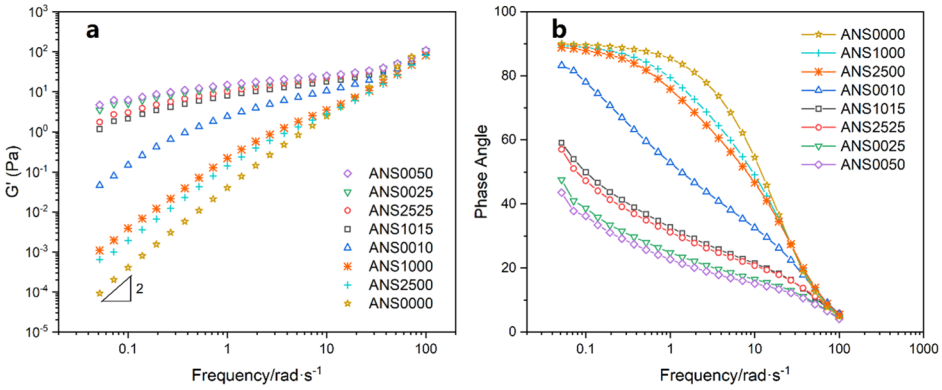

Figure 5. Storage (G') (a) and phase angle (b) as a function of frequency at 1.2 wt % polymer concentration.

the steric hindrance and strong intramolecular Coulomb repulsion may, to some extent, offset the "polyelectrolyte effect" encountered by linear ones. This makes the measurement and comparison of intrinsic viscosity in a salt-free solution possible. Attempts were made with the Martin equation in the present research, and results are shown in Figure 3 (part of the data for $\ln(\eta_{red})$ versus concentration were shown in Figure S5 for clarity).

As can be observed in Figure 3b, with the same molar ratio in the copolymer, a SAMPS unit can expand the hydrodynamic volume of the grafted copolymer more significantly than the NIPAM unit because of the Coulomb repulsion forces. The changes in the intrinsic viscosity between grafted AM/SAMPS bi-component copolymers also signify an optimum SAMPS intake (25 mol %) in the composition. Interestingly, compared to the increase of intrinsic viscosity between ANS0010 and ANS1015, a decrease can be observed between ANS0025 and ANS2525, which indicates a negative influence of the NIPAM unit on the hydrodynamic volume of the copolymer. This trend is in agreement with the sequence of the low shear rate viscosity ($\gamma < 10\ s^{-1}$ in Figure 4a) of copolymers which is more related with the hydrodynamic volume and excluded volume.[49−51] One may argue that the (co)polymer concentration is still too high to show the "polyelectrolyte effect". However, this effect can be observed in the same concentration range according to one previous report on spherical polyelectrolytes.[52] Nevertheless, the validity of measuring the intrinsic viscosity of synthesized starch-based branched polyelectrolytes with the Martin equation in salt-free water still needs further investigation.

The influence of chain composition on solution viscosity as a function of shear rate was also evaluated at the same polymer concentration, the result of which is shown in Figure 4a. It is clear that because of the extended molecular chains resulting from the Coulomb repulsion forces, the viscosity of AM/SAMPS bi-component copolymers is much higher than that of AM/NIPAM bi-component copolymers, especially in the low shear rate region. It is also noticed that copolymers with a higher SAMPS intake (e.g., > 25 mol %, ANS0050) are more shear sensitive at a high shear rate ($>10\ s^{-1}$) than other copolymers. This is attributed to the weak chain entanglement because of the Coulomb repulsion forces. Furthermore, these data were also fitted with the Carreau−Yasuda model (see the Materials and Methods section) to study the influence of chain composition on the copolymer relaxation time (λ).[9,35,36] As indicated in Figure 4b, a higher SAMPS intake results in higher λ values, thus, the lower critical shear thinning rate ($1/\lambda$) should be observed in the flow curve. This is in line with Figure 4a which shows a shift in the onset of shear thinning behavior toward lower shear rate regions. In the case of an AM/NIPAM/SAMPS tri-component copolymer, high NIPAM intake, like its effect on the intrinsic viscosity, reduces the relaxation time which means the copolymer solution is less shear sensitive (comparing the λ of ANS0025, ANS2525 in Figure 4b and corresponding flow curve in Figure 4a). This may be related to the intermolecular association because of the high ratio of NIPAM units.

Besides viscosity, the viscoelastic property also affects the performance of polymers in applications such as improving the sweep efficiency in EOR.[53] The influence of composition on the viscoelastic properties of the copolymers is shown in Figure 5 (for clarity the plot of loss modulus vs frequency is shown in Figure S6). In Figure 5a, in the terminal zone (low frequency region), typical Maxwell flow behavior with G' proportional to ω^2 (slope = 2) and G'' directly proportional to the angular frequency (ω) (slope = 1) can be observed for samples with low SAMPS intake.[54] For copolymers with high SAMPS intake (e.g., > 15 mol %, ANS1015), deviation in the slope from the Maxwell model is observed which suggests intermolecular entanglement.[49] Similar to the viscosity profile shown in the flow curve in Figure 4a, both the storage modulus (G') and the loss modulus (G'') of SAMPS-containing copolymers increased more significantly ($\omega < 20$ rad/s) compared with those of AM/NIPAM bi-component copolymers. The same trend can also be observed in the change of solution elastic response as indicated by the phase angles at equal copolymer concentrations (Figure 5b). All these results, such as the intrinsic viscosity and viscosity versus shear rate curve (vide supra), indicate an optimum SAMPS ratio (25 mol %) in the copolymers as well.

As evidenced by the results shown above, at a high molar ratio the NIPAM intake displays a negative influence on the rheology performance of the SAMPS copolymer in fresh water. In application areas such as EOR, an inorganic electrolyte present in the solution can screen the Coulomb forces which may result in different rheology behavior. Thus, the influence of salt and NIPAM intake on the viscosity of the copolymer was also studied in saline water with different NaCl concentration. As shown in Figure 6, all the SAMPS copolymers display higher viscosity than that of AM/NIPAM bi-component copolymers (optimally, 220 mPa·s, see ref 12) when the SAMPS intake is high enough (e.g., > 10 mol %). Comparison between different SAMPS-containing copolymers also indicates 25% is the optimum SAMPS ratio for their saline

https://dx.doi.org/10.1021/acs.iecr.9b06893
Ind. Eng. Chem. Res. 2020, 59, 10847−10856

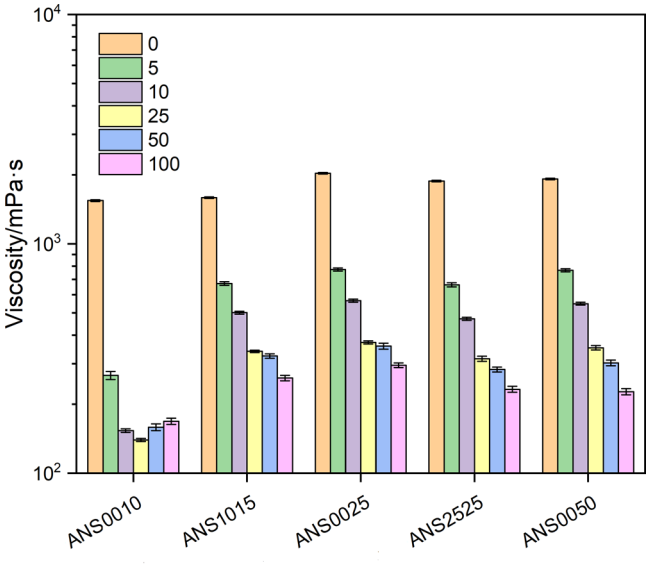

Figure 6. Viscosity (γ = 10 s^{-1}) as a function of salinity (unit in kilo ppm) for starch-based graft copolymers (1.0 wt %).

resistance in viscosity: while a lower ratio is not enough to effectively break down the hydrogen bond between AM units in saline water (ANS0010), a higher ratio makes the hydrodynamic volume of the copolymers more sensitive to salt (ANS0050). The saline sensitivity of ANS0050 is further proved when comparing its viscosity with that of ANS1015 and ANS0025 when the salinity is higher than 50,000 ppm. In the case of AM/NIPAM/SAMPS tri-component copolymers, the incorporation of the NIPAM unit leads to a lower viscosity which is related to the intramolecular association of NIPAM units at a high salt concentration because of the collapse of the macromolecule (comparing the viscosity of ANS0025 and ANS2525 in Figure 6).

Besides the influence of NIPAM on the room temperature rheology, the thermo-thickening behavior of the NIPAM copolymer is also of interest for applications such as EOR. According to our previous report, the thermo-thickening behavior is not only affected by the intake of the NIPAM unit, but also by the strong intramolecular hydrogen bond in the waxy starch-based highly branched AM copolymer.[12] In the present research, the Coulomb repulsion between SAMPS units breaks down the intramolecular hydrogen bond and also hinders the intermolecular association of NIPAM units in fresh and low salinity (<25,000 ppm) water. As a result, no thermo-thickening behavior is observed at a shear rate of 1 s^{-1} in group A of Figure 7a. With the increasing salinity, charges on the polymer chains are screened effectively which makes the hydrophobic association of NIPAM units possible. This is proved by the thermo-thickening behavior indicated by group B (Figure 7a) and the more obvious increment of viscosity in a higher salinity solution (group C, Figure 7a). At a higher shear rate (γ = 3 s^{-1}), the hydrophobic association can be disrupted, as the result of which thermo-thickening is only observed at really high salinity (more hydrophobic association) as can be seen in Figure 7b. At an even higher shear rate, for example, the average shear rate in porous media (γ = 10 s^{-1}) as reported, no thermo-thickening behavior of AM/NIPAM/SAMPS tri-component copolymers is observed in Figure 7c,d.[55,56] The viscosity−temperature profiles of different copolymers are also shown in the same graph for comparison. As can be observed, SAMPS-containing bi-component

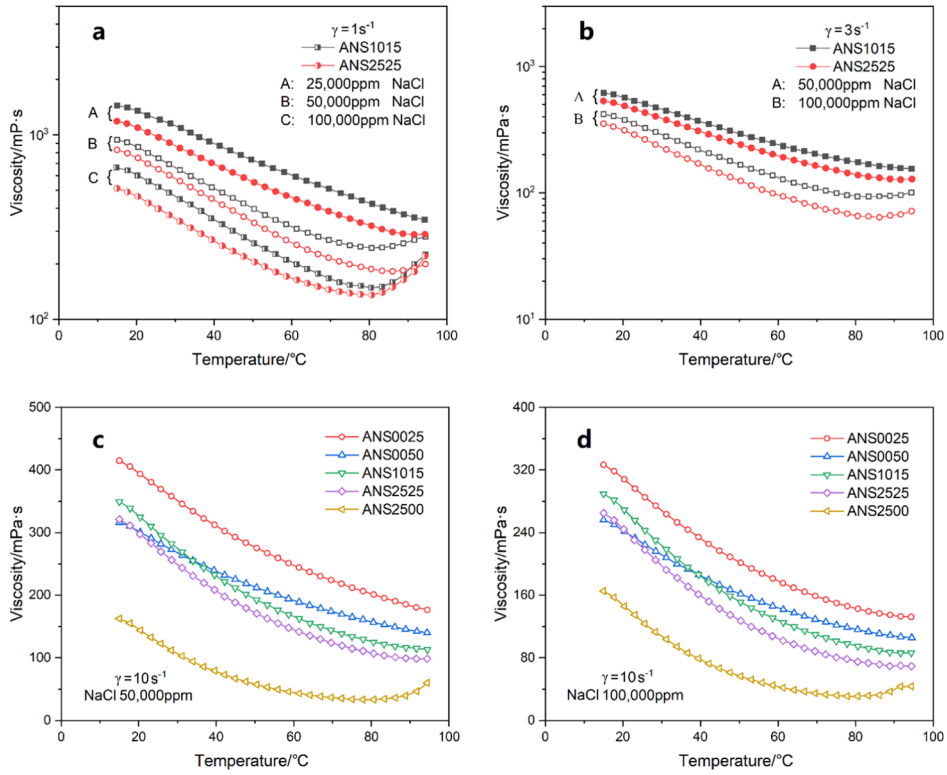

Figure 7. Viscosity vs temperature of waxy potato starch-based AM/SAMPS/NIPAM copolymers in saline water at different shear rates (1.0 wt % copolymer concentration).

https://dx.doi.org/10.1021/acs.iecr.9b06893
Ind. Eng. Chem. Res. 2020, 59, 10847−10856

copolymers display better temperature and saline resistance compared with tri-component copolymers. This is more obvious in the case of ANS0050 which has a lower viscosity under room temperature compared with other copolymers but displays higher viscosity than AM/NIPAM/SAMPS tri-component copolymers at high temperature and salinity (e.g., above 40 °C and 50,000 ppm NaCl). This may also be related to its higher charge density in comparison with other copolymers. Considering the higher viscosity of ANS2525 relative to that of ANS1015 in fresh water (Figure 6), the intake of a high mole ratio of the NIPAM unit in the copolymer again proved to play a negative role on the saline resistance property of the copolymer in a wide temperature range.

4. CONCLUSIONS

In this work, a water-soluble waxy potato starch macroinitiator was homogeneously synthesized in DMAc. A series of random copolymers of AM, SAMPS, and NIPAM were then grafted from the macroinitiator via aqueous Cu^0-mediated living radical polymerization (Cu^0-mediated LRP) at room temperature. The mole ratios of SAMPS and NIPAM were varied in the range of 0−50 and 0−25%, respectively, to investigate the influence of chain composition on copolymers' aqueous rheological properties as well as their thermo-responsive properties. Because of the negatively charged side groups, waxy potato starch-based AM/SAMPS bi-component copolymers displayed much higher viscosity than AM/NIPAM bi-component copolymers in saline solution. Comparison of intrinsic viscosity, viscosity profile at different shear rates, and salinity between different copolymers indicated an optimum SAMPS ratio (25 mol %) for the balanced performance of viscosity and salt resistance. The intake of a high ratio of the NIPAM unit undermines the thickening ability of AM/NIPAM/SAMPS tri-component copolymers) in both fresh and saline water because of hydrophobic association. In a high salinity solution, the hydrodynamic volume of the macromolecule collapses because of the screening effect of salt on the charged SAMPS units. As the result, thermo-thickening behavior can be observed at low shear rates ($\gamma \leq 3\ s^{-1}$) because of hydrophobic association. At a higher shear rate, the thermo-thickening behavior disappears because of the disruption of association.

■ ASSOCIATED CONTENT

Supporting Information

The Supporting Information is available free of charge at https://pubs.acs.org/doi/10.1021/acs.iecr.9b06893.

Synthesis of waxy potato StBr and St-g-PAM, illustration for the highly branched structure of amylopectin and its copolymer, FT-IR spectra of StBr with different DS, ^{1}H-NMR, ^{13}C-NMR, and gHSQC spectra of StBr (DS = 0.15) in D_2O, elemental analysis result of starch-based graft copolymer, GPC traces of (co)polymers cleaved from a starch backbone, reduced viscosity as a function of polymer concentration (Martin equation), and loss modulus versus frequency of starch-based copolymer (1.2 wt %) (PDF)

■ AUTHOR INFORMATION

Corresponding Author

Francesco Picchioni − *Engineering and Technology Institute Groningen, University of Groningen, 9747AG Groningen, The Netherlands;* orcid.org/0000-0002-8232-2083; Phone: +31-050-363-4333; Email: f.picchioni@rug.nl

Authors

Yifei Fan − *Engineering and Technology Institute Groningen, University of Groningen, 9747AG Groningen, The Netherlands*

Ranjita K. Bose − *Engineering and Technology Institute Groningen, University of Groningen, 9747AG Groningen, The Netherlands*

Complete contact information is available at: https://pubs.acs.org/10.1021/acs.iecr.9b06893

Funding

This work was performed under the financial support from the China Scholarship Council (CSC).

Notes

The authors declare no competing financial interest.

■ ACKNOWLEDGMENTS

We thank the financial support from the China Scholarship Council (CSC) (grant number: 201406380107). We also thank Avebe (Veendam, The Netherlands) for the donation of the waxy potato starch.

■ REFERENCES

(1) Romero-Zerón, L. Advances in enhanced oil recovery processes. *Introduction to Enhanced Oil Recovery (EOR) Processes and Bioremediation of Oil-Contaminated Sites*; InTech, 2012.

(2) Wei, B.; Romero-Zerón, L.; Rodrigue, D. Oil displacement mechanisms of viscoelastic polymers in enhanced oil recovery (EOR): a review. *J. Pet. Explor. Prod. Technol.* **2013**, *4*, 113−121.

(3) IEA. *Key World Energy Statistics*; International Energy Agency Paris, 2015.

(4) Hashmet, M. R.; AlSumaiti, A. M.; Qaiser, Y.; AlAmeri, W. S. Laboratory Investigation and Simulation Modeling of Polymer Flooding in High-Temperature, High-Salinity Carbonate Reservoirs. *Energy Fuels* **2017**, *31*, 13454−13465.

(5) Ge, J.; Wang, Y. Surfactant Enhanced Oil Recovery in a High Temperature and High Salinity Carbonate Reservoir. *J. Surfactants Deterg.* **2015**, *18*, 1043−1050.

(6) Strand, S.; Puntervold, T.; Austad, T. Effect of Temperature on Enhanced Oil Recovery from Mixed-Wet Chalk Cores by Spontaneous Imbibition and Forced Displacement Using Seawater. *Energy Fuels* **2008**, *22*, 3222−3225.

(7) Zheng, J.; Chen, B.; Thanyamanta, W.; Hawboldt, K.; Zhang, B.; Liu, B. Offshore produced water management: A review of current practice and challenges in harsh/Arctic environments. *Mar. Pollut. Bull.* **2016**, *104*, 7−19.

(8) Robinson, D. Oil and gas: Treatment of produced waters for injection and reinjection. *Filtrat. Separ.* **2013**, *50*, 36−43.

(9) Wever, D. A. Z.; Polgar, L. M.; Stuart, M. C. A.; Picchioni, F.; Broekhuis, A. A. Polymer Molecular Architecture As a Tool for Controlling the Rheological Properties of Aqueous Polyacrylamide Solutions for Enhanced Oil Recovery. *Ind. Eng. Chem. Res.* **2013**, *52*, 16993−17005.

(10) Wever, D. A. Z.; Picchioni, F.; Broekhuis, A. A. Branched polyacrylamides: Synthesis and effect of molecular architecture on solution rheology. *Eur. Polym. J.* **2013**, *49*, 3289−3301.

(11) Wever, D. A. Z.; Riemsma, E.; Picchioni, F.; Broekhuis, A. A. Comb-like thermoresponsive polymeric materials: Synthesis and

effect of macromolecular structure on solution properties. *Polymer* **2013**, *54*, 5456−5466.
(12) Fan, Y.; Boulif, N.; Picchioni, F. Thermo-Responsive Starch-g-(PAM-co-PNIPAM): Controlled Synthesis and Effect of Molecular Components on Solution Rheology. *Polymers* **2018**, *10*, 92.
(13) Zobel, H. F. Molecules to Granules: A Comprehensive Starch Review. *Starch—Stärke* **1988**, *40*, 44−50.
(14) Jane, J.-l. Starch: Structure and Properties. In *Chemical and functional properties of food saccharides*; Tomasik, P., Ed.; CRC Press, 2004.
(15) Yoo, S.; Jane, J.-l. Molecular weights and gyration radii of amylopectins determined by high-performance size-exclusion chromatography equipped with multi-angle laser-light scattering and refractive index detectors. *Carbohydr. Polym.* **2002**, *49*, 307−314.
(16) Li, X. e.; Xu, Z.; Yin, H.; Feng, Y.; Quan, H. Comparative Studies on Enhanced Oil Recovery: Thermoviscosifying Polymer Versus Polyacrylamide. *Energy Fuels* **2017**, *31*, 2479−2487.
(17) Seright, R. S.; Campbell, A.; Mozley, P.; Han, P. Stability of Partially Hydrolyzed Polyacrylamides at Elevated Temperatures in the Absence of Divalent Cations. *SPE J.* **2010**, *15*, 341−348.
(18) Wang, F.; Jeon, J.-H.; Kim, S.-J.; Park, J.-O.; Park, S. An eco-friendly ultra-high performance ionic artificial muscle based on poly(2-acrylamido-2-methyl-1-propanesulfonic acid) and carboxylated bacterial cellulose. *J. Mater. Chem. B* **2016**, *4*, 5015−5024.
(19) Zhao, P.; Gao, B.; Xu, S.; Kong, J.; Ma, D.; Shon, H. K.; Yue, Q.; Liu, P. Polyelectrolyte-promoted forward osmosis process for dye wastewater treatment − Exploring the feasibility of using polyacrylamide as draw solute. *Chem. Eng. J.* **2015**, *264*, 32−38.
(20) Ge, Q.; Wang, P.; Wan, C.; Chung, T.-S. Polyelectrolyte-promoted forward osmosis-membrane distillation (FO-MD) hybrid process for dye wastewater treatment. *Environ. Sci. Technol.* **2012**, *46*, 6236−6243.
(21) Sahiner, N.; Seven, F. Energy and environmental usage of super porous poly(2-acrylamido-2-methyl-1-propan sulfonic acid) cryogel support. *RSC Adv.* **2014**, *4*, 23886−23897.
(22) Qi, L.; Wanfen, P.; Yabo, W.; Tianhong, Z. *Synthesis and Assessment of a Novel AM-co-AMPS Polymer for Enhanced Oil Recovery (EOR)*; IEEE, 2013; pp 997−1000.
(23) Song, H.; Zhang, S.-F.; Ma, X.-C.; Wang, D.-Z.; Yang, J.-Z. Synthesis and application of starch-graft-poly(AM-co-AMPS) by using a complex initiation system of CS-APS. *Carbohydr. Polym.* **2007**, *69*, 189−195.
(24) Lee, J.; Moesari, E.; Dandamudi, C. B.; Beniah, G.; Chang, B.; Iqbal, M.; Fei, Y.; Zhou, N.; Ellison, C. J.; Johnston, K. P. Behavior of Spherical Poly(2-acrylamido-2-methylpropanesulfonate) Polyelectrolyte Brushes on Silica Nanoparticles up to Extreme Salinity with Weak Divalent Cation Binding at Ambient and High Temperature. *Macromolecules* **2017**, *50*, 7699−7711.
(25) Cheng, Y.; Zhao, M.; Zheng, C.; Guo, S.; Li, X.; Zhang, Z. Water-Dispersible Reactive Nanosilica and Poly(2-acrylamido-2-methyl-1-propanesulfonic acid sodium) Nanohybrid as Potential Oil Displacement Agent for Enhanced Oil Recovery. *Energy Fuels* **2017**, *31*, 6345−6351.
(26) Zou, W.; Liu, X.; Yu, L.; Qiao, D.; Chen, L.; Liu, H.; Zhang, N. Synthesis and Characterization of Biodegradable Starch-Polyacrylamide Graft Copolymers Using Starches with Different Microstructures. *J. Polym. Environ.* **2012**, *21*, 359−365.
(27) Jones, G. R.; Li, Z.; Anastasaki, A.; Lloyd, D. J.; Wilson, P.; Zhang, Q.; Haddleton, D. M. Rapid Synthesis of Well-Defined Polyacrylamide by Aqueous Cu(0)-Mediated Reversible-Deactivation Radical Polymerization. *Macromolecules* **2016**, *49*, 483−489.
(28) Masci, G.; Giacomelli, L.; Crescenzi, V. Atom transfer radical polymerization of sodium2-acrylamido-2-methylpropanesulfonate. *J. Polym. Sci., Part A: Polym. Chem.* **2005**, *43*, 4446−4454.
(29) McCullough, L. A.; Dufour, B.; Matyjaszewski, K. Incorporation of poly(2-acrylamido-2-methyl-N-propanesulfonic acid) segments into block and brush copolymers by ATRP. *J. Polym. Sci., Part A: Polym. Chem.* **2009**, *47*, 5386−5396.
(30) Nikolaou, V.; Simula, A.; Droesbeke, M.; Risangud, N.; Anastasaki, A.; Kempe, K.; Wilson, P.; Haddleton, D. M. Polymerisation of 2-acrylamido-2-methylpropane sulfonic acid sodium salt (NaAMPS) and acryloyl phosphatidylcholine (APC) via aqueous Cu(0)-mediated radical polymerisation. *Polym. Chem.* **2016**, *7*, 2452−2456.
(31) Zhang, C.; Liu, R.; Xiang, J.; Kang, H.; Liu, Z.; Huang, Y. Dissolution mechanism of cellulose in N,N-dimethylacetamide/lithium chloride: revisiting through molecular interactions. *J. Phys. Chem. B* **2014**, *118*, 9507−9514.
(32) El Seoud, O.; Nawaz, H.; Arêas, E. Chemistry and applications of polysaccharide solutions in strong electrolytes/dipolar aprotic solvents: an overview. *Molecules* **2013**, *18*, 1270−1313.
(33) Icke, R. N.; Wisegarver, B. B.; Alles, G. A. *β*-Phenylethyldimethylamine. *Org. Synth.* **1945**, *25*, 89−92.
(34) Masuelli, M. A.; Sansone, M. G. Hydrodynamic Properties of Gelatin-Studies from Intrinsic Viscosity Measurements. *Products and Applications of Biopolymers*; InTech, 2012.
(35) Yasuda, K.; Armstrong, R. C.; Cohen, R. E. Shear flow properties of concentrated solutions of linear and star branched polystyrenes. *Rheol. Acta* **1981**, *20*, 163−178.
(36) Carreau, P. J. Rheological equations from molecular network theories. *Trans. Soc. Rheol.* **1972**, *16*, 99−127.
(37) Goto, A.; Fukuda, T. Kinetics of living radical polymerization. *Prog. Polym. Sci.* **2004**, *29*, 329−385.
(38) Gao, Y.; Zhao, T.; Zhou, D.; Greiser, U.; Wang, W. Insights into relevant mechanistic aspects about the induction period of Cu(0)/Me(6)TREN-mediated reversible-deactivation radical polymerization. *Chem. Commun.* **2015**, *51*, 14435−14438.
(39) Beattie, D. A.; Addai-Mensah, J.; Beaussart, A.; Franks, G. V.; Yeap, K.-Y. In situ particle film ATR FTIR spectroscopy of poly (N-isopropyl acrylamide) (PNIPAM) adsorption onto talc. *Phys. Chem. Chem. Phys.* **2014**, *16*, 25143−25151.
(40) Zhu, J.; Tian, M.; Hou, J.; Wang, J.; Lin, J.; Zhang, Y.; Liu, J.; Van der Bruggen, B. Surface zwitterionic functionalized graphene oxide for a novel loose nanofiltration membrane. *J. Mater. Chem. A* **2016**, *4*, 1980−1990.
(41) Achilleos, M.; Demetriou, M.; Marinica, O.; Vekas, L.; Krasia-Christoforou, T. An innovative synthesis approach toward the preparation of structurally defined multiresponsive polymer (co)-networks. *Polym. Chem.* **2014**, *5*, 4365.
(42) Li, H.; Miao, H.; Gao, Y.; Li, H.; Chen, D. Efficient synthesis of narrowly dispersed amphiphilic double-brush copolymers through the polymerization reaction of macromonomer micelle emulsifiers at the oil−water interface. *Polym. Chem.* **2016**, *7*, 4476−4485.
(43) Rabea, A.; Zhu, S. Modeling the Influence of Diffusion-Controlled Reactions and Residual Termination and Deactivation on the Rate and Control of Bulk ATRP at High Conversions. *Polymers* **2015**, *7*, 819−835.
(44) Arvidson, S. A.; Rinehart, B. T.; Gadala-Maria, F. Concentration regimes of solutions of levan polysaccharide from Bacillus sp. *Carbohydr. Polym.* **2006**, *65*, 144−149.
(45) Lee, J.; Tripathi, A. Intrinsic viscosity of polymers and biopolymers measured by microchip. *Anal. Chem.* **2005**, *77*, 7137−7147.
(46) Kulicke, W.-M.; Clasen, C. *Viscosimetry of Polymers and Polyelectrolytes*; Springer Science & Business Media, 2013.
(47) Badiger, M. V.; Gupta, N. R.; Eckelt, J.; Wolf, B. A. Intrinsic Viscosity of Aqueous Solutions of Carboxymethyl Guar in the Presence and in the Absence of Salt. *Macromol. Chem. Phys.* **2008**, *209*, 2087−2093.
(48) Xiong, X.; Wolf, B. A. Intrinsic viscosities of polyelectrolytes: specific salt effects and viscometric master curves. *Soft Matter* **2014**, *10*, 2124−31.
(49) Gupta, R. K. *Polymer and composite Rheology*; CRC Press, 2000.
(50) Macosko, C. W. *Rheology: Principles, Measurements, and Applications*; Wiley-vch, 1994.

https://dx.doi.org/10.1021/acs.iecr.9b06893
Ind. Eng. Chem. Res. 2020, 59, 10847−10856

(51) Shawki, S. M.; Hamielec, A. E. The effect of shear rate on the molecular weight determination of acrylamide polymers from intrinsic viscosity measurements. *J. Appl. Polym. Sci.* **1979**, *23*, 3323−3339.
(52) Antonietti, M.; Briel, A.; Förster, S. Intrinsic viscosity of small spherical polyelectrolytes: Proof for the intermolecular origin of the polyelectrolyte effect. *J. Chem. Phys.* **1996**, *105*, 7795−7807.
(53) Zhu, D.; Zhang, J.; Han, Y.; Wang, H.; Feng, Y. Laboratory Study on the Potential EOR Use of HPAM/VES Hybrid in High-Temperature and High-Salinity Oil Reservoirs. *J. Chem.* **2013**, *2013*, 1−8.
(54) Picout, D. R.; Ross-Murphy, S. B. *Thermoreversible and Irreversible Physical Gels from Biopolymers*; Marcel Dekker, Inc.: New York, 2002.
(55) Berg, S.; van Wunnik, J. Shear Rate Determination from Pore-Scale Flow Fields. *Transp. Porous Media* **2017**, *117*, 229−246.
(56) Niu, Y.; Jian, O.; Zhu, Z.; Wang, G.; Sun, G.; Shi, l., Research on Hydrophobically Associating Water-soluble Polymer Used for EOR. *SPE International Symposium on Oilfield Chemistry*; Society of Petroleum Engineers: Houston, Texas, 2001.

https://dx.doi.org/10.1021/acs.iecr.9b06893
Ind. Eng. Chem. Res. 2020, 59, 10847−10856